MADRID
inter.noise 2019
June 16 - 19
NOISE CONTROL FOR A BETTER ENVIRONMENT

Active control for panel Transmission Loss improvement

Baro, Simone[1]
Department of Mechanical Engineering, Politecnico di Milano
Via La Masa 1, Milano, Italy

Corradi, Roberto[2]
Department of Mechanical Engineering, Politecnico di Milano
Via La Masa 1, Milano, Italy

Ripamonti, Francesco[3]
Department of Mechanical Engineering, Politecnico di Milano
Via La Masa 1, Milano, Italy

ABSTRACT

Vibroacoustic comfort is becoming more and more a fundamental requirement for the development of new products in both transport and civil engineering. The demand for improved performance is particularly challenging due to the increasing employment of lightweight composite materials in aircraft panels, vehicle body structures and building partitions. Indeed, composite materials are widely used for their high stiffness-to-weight ratio, although this characteristic, beside a generally low structural damping, implies poor vibroacoustic performances. Viscoelastic or massive treatments are commonly employed to mitigate these drawbacks. With reference to the airborne path, the application of active control is here investigated for improving the panel Transmission Loss at low frequency, where passive treatments are less effective. A time domain model for predicting the Transmission Loss in case of single or diffuse field incidence is presented. The model is validated against experimental measurements performed in a double reverberation chamber. Then, active control is introduced into the model and its effectiveness in increasing the panel acoustic insulation is verified.

Keywords: Transmission Loss, Active Vibration Control, Reverberation Chamber
I-INCE Classification of Subject Number: 33, 42

1. INTRODUCTION

The industry interest in lightweight composite materials and structures is constantly increasing together with the range of applications where such materials are employed. Airplane and train flooring, cabin structures and wall partitions are just some

[1] Simone.baro@polimi.it
[2] Roberto.corradi@polimi.it
[3] Francesco.ripamonti@polimi.it

examples of systems where lightweight materials are used thanks to their high stiffness-to-weight ratio. This characteristic, however, generally implies poor vibro-acoustic performances, leading to the need of proper countermeasures. With reference to the airborne path, several solutions have been investigated in the literature, ranging from the modelling of multilayer panels eventually including noise control treatments [1-5] to the application of an actuating system for active noise control [6-13]. A review of the state-of-the-art of active vibration and noise suppression was done by Aridogan and Basdogan [11] and the linear-quadratic regulator (LQR) was studied by Balamurugan and Narayanan [12] for distributed sensors and actuators.

The present paper deals with the application of an active control system for enhancing the Transmission Loss (TL) of lightweight panels. In particular, the interest is in the low frequency range where passive solutions, such as massive and damping treatments, are less effective. As a first step, a transmission model for assessing the TL of thin panels is developed similarly to the one presented by Lu and Xin [4]. A validation of the current approach is then provided by comparing the numerically predicted TL against that measured in a double reverberation chamber [14]. An LQR control is then designed and its effectiveness assessed by numerical simulations of an acoustically excited aluminium panel.

2. TRANSMISSION LOSS MODEL

The investigation of the Transmission Loss performance of a panel is here investigated considering a thin in-plane isotropic flat rectangular plate featured by a constant thickness. The panel can be characterized by an arbitrary stacking sequence as far as transversally stiff materials are used realizing an in-phase motion of the outer skins. As schematically represented in Figure 1, the panel has side dimensions a and b, and thickness h. The plate is assumed to be in an infinite rigid baffle, with arbitrary boundary conditions being the present approach applicable for any kind of constrains, as far as analytical or numerical definition of the mode shapes is available. The panel is confined on both sides of the plate by the fluid termed 1 and 2 having properties ρ_i, c_i and k_i (for $i = 1, 2$), corresponding to the fluid density, sound speed and characteristic wave number respectively.

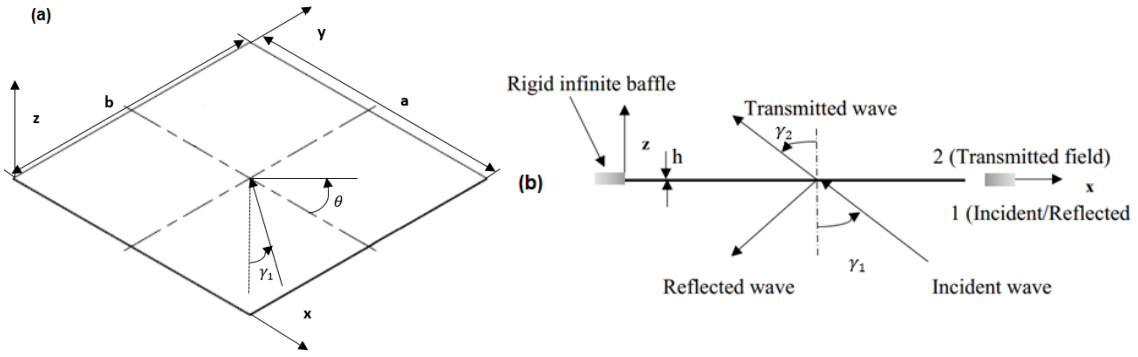

Figure 1 – Schematic view of the sound transmission through a panel immersed in air: (a) overall view; (b) view in the x-y plane [4]

As shown in Figure 1, the middle thickness plane coincides with the x-y plane whereas the z-axis points in the thickness direction. A plane wave acoustic excitation is

considered on the bottom side of the panel (z<0) with incidence angle γ_1 and azimuth angle θ. The acoustic excitation induces a vibration of the plate that in turn radiates sound on both sides, realizing an incident/reflected field for z<0 and a transmitted field for z>0. Considering the pressure fluctuations on both sides of the plate, the equation of motion of the plate can be described according to the Kirchhoff's theory as

$$B\nabla^4 w(x,y,t) + m\frac{\partial^2 w}{\partial t^2}(x,y,t) = p_1(x,y,0,t) - p_2(x,y,0,t) \tag{1}$$

where the pressure fields act as forcing terms on the right-hand side of Equation 1 being $p_1(x,y,0,t)$ the pressure field formed by the incident and reflected waves at the plate surface and similarly $p_2(x,y,0,t)$ accounting for the pressure filed realized by the trasmitted wave solely. In Equation 1, *B* is the panel bending stiffness, *m* is the surface density whereas *w* is the plate displacement in the z positive direction. Considering the relationship $p_i = \rho_i \frac{\partial \phi_i}{\partial t}$ (for $i = 1, 2$), the velocity potentials ϕ_i on both sides of the plate are defined as

$$\phi_1(x,y,z,t) = I_0 e^{-j(k_{1x}x + k_{1y}y + k_{1z}z - \omega t)} + \beta_0 e^{-j(k_{1x}x + k_{1y}y - k_{1z}z - \omega t)} \tag{2a}$$

$$\phi_2(x,y,z,t) = \varepsilon_0 e^{-j(k_{2x}x + k_{2y}y + k_{2z}z - \omega t)} \tag{2b}$$

where ω is the angular frequency and I_0, β_0 and ε_0 are the amplitudes of the incident, reflected and transmitted plane waves respectively. Assuming the same fluid on both sides, the γ_i angles are equal as well as the wavenumber components k_{ix}, k_{iy} and k_{iz}. Equation 2 can be rewritten by expanding the velocity fields over planes parallel to x-y (see Figure 1) as a linear combination of the panel mode shapes $\varphi_i(x,y)$ as

$$\Phi_1(x,y,z;t) = \sum_{i=1}^{\infty} I_i \varphi_i(x,y) e^{-j(k_{1z}z - \omega t)} + \sum_{i=1}^{\infty} \beta_i \varphi_i(x,y) e^{-j(-k_{1z}z - \omega t)} \tag{3a}$$

$$\Phi_2(x,y,z;t) = \sum_{i=1}^{\infty} \varepsilon_i \varphi_i(x,y) e^{-j(k_{2z}z - \omega t)} \tag{3b}$$

where each modal amplitude (I_i, β_i, ε_i) is related to the plane wave amplitudes (I_0, β_0, ε_0) as

$$\lambda_i = \int_0^b \int_0^a \lambda_0 e^{-j(k_{1x}x + k_{1y}y)} \varphi_i(x,y)\, dxdy \tag{4}$$

and where λ refers to any generic amplitude (incident, reflected or transmitted). Imposing the same velocity for the fluid and the plate at the interface and describing the dynamic panel displacement through the superposition, so as

$$w(x,y;t) = \sum_{i=1}^{\infty} \varphi_i q_i(t) = \sum_{i=1}^{\infty} \varphi_i q_{0,i} e^{j\omega t} \tag{5}$$

and the equation of motion in the generalized coordinate $q_{0,i}$ becomes

$$\left[-m\omega^2 + 2j\omega\rho\frac{\omega}{k_z} + m{\omega_i}^2\right] q_{0,i} = 2j\omega\rho I_i \tag{6}$$

Equation 6 shows the effect of the fluid-structure coupling realizing equivalent damping terms depending on the fluid properties and incident angle. Gathering the first N modal coordinates and their time derivatives in the vectors $\underline{q}$, $\underline{\dot{q}}$ and $\underline{\ddot{q}}$ respectively, the panel equation of motion is derived through Equation 5 as

$$[M]\underline{\ddot{q}} + [C_F]\underline{\dot{q}} + [K]\underline{q} = 2\rho\underline{\dot{I}} \tag{7}$$

where $[M]$ and $[K]$ are the modal mass and stiffness matrices. By solving Equation 6, for a given incident wave, the pressure on both sides can be fully determined and the Transmission Loss (TL) can be computed

$$\tau = \Pi_2/\Pi_1 \quad \rightarrow \quad TL = 10\log(1/\tau) \tag{8}$$

where τ is the transmission coefficient [7] while Π_1 and Π_2 are the acoustic powers defined as

$$\Pi_1 = \frac{1}{T}\int \iint \frac{\rho}{c}\left(2I_0 e^{-j(k_{1x}x+k_{1y}y)} j\omega e^{j\omega t} - \frac{c}{\cos(\gamma_1)}\underline{\varphi}^T\underline{\dot{q}}\right)^2 dA\, dt \tag{9a}$$

$$\Pi_2 = \frac{1}{T}\int \iint \frac{\rho c}{\cos(\gamma_2)}\underline{\varphi}^T\underline{\dot{q}}\, dA\, dt \tag{9b}$$

Combining the transmission coefficients computed for different incident and azimuth angles, the transmission coefficient of the panel excited by a diffuse acoustic field is derived as

$$\tau_{diff} = \frac{\int_0^{\gamma_1 max}\int_0^{2\pi} \tau(\gamma_1,\theta,\omega)\sin(\gamma_1)\cos(\gamma_1)\, d\theta d\gamma_1}{\int_0^{\gamma_1 max}\int_0^{2\pi} \sin(\gamma_1)\cos(\gamma_1)\, d\theta d\gamma_1} \tag{10}$$

3. EXPERIMENTAL VALIDATION

In order to validate the model presented in the previous section, Transmission Loss tests have been performed at CSI S.p.A according to the ISO standard 10140-2 [14]. The testing facility consists of two coupled reverberation chambers, i.e. a source chamber and a receiving one, sharing an aperture where a concrete frame is installed. The test specimen is then positioned in a predisposed opening in the concrete frame and sealed on both sides in order to avoid leakages that would invalidate the measurement. Figure 2 shows the source and the receiving chambers.

Figure 2 – Transmission Loss facility: source (left) and receiving (right) reverberant chambers.

In the source chamber a sound source is moved on a linear guide in order to assure sound field diffuseness. Measurements with a moving microphone are performed in order to evaluate the space-averaged sound pressure level both in the source and receiving chamber, while the sound source in the source chamber is on. The Transmission Loss is then estimated according to [14] as

$$TL = L_{pS} - L_{pR} + \log(S/A) \tag{11}$$

where L_{pS} and L_{pR} are the average Sound Pressure Levels in the source and receiving chamber respectively, S is specimen surface and A is the equivalent sound absorption area in the receiving chamber. The latter equivalent sound absorption area is estimated from the reverberation time in the receiving chamber. Indeed, prior to each measurement and after the test specimen is mounted in the frame, the reverberation time of the receiving chamber is evaluated by measuring the Sound Pressure Level drop when a sound source on the receiving chamber side is suddenly switched off.

Figure 3 compares the experimental TL and numerical prediction, based on the model presented in the previous section (Equation 10), for an aluminium panel of dimensions a=1.240 m, b=0.990 m, s=0.005 m and properties E=69 GPa (Young's modulus), ν=0.3 (Poisson coefficient) and m=13.71 kg/m^2 (mass per unit area). Simply supported boundary conditions have been assumed for the panel. The air domain on both sides is considered with ρ=1.22 kg/m^3 and c=343 m/s.

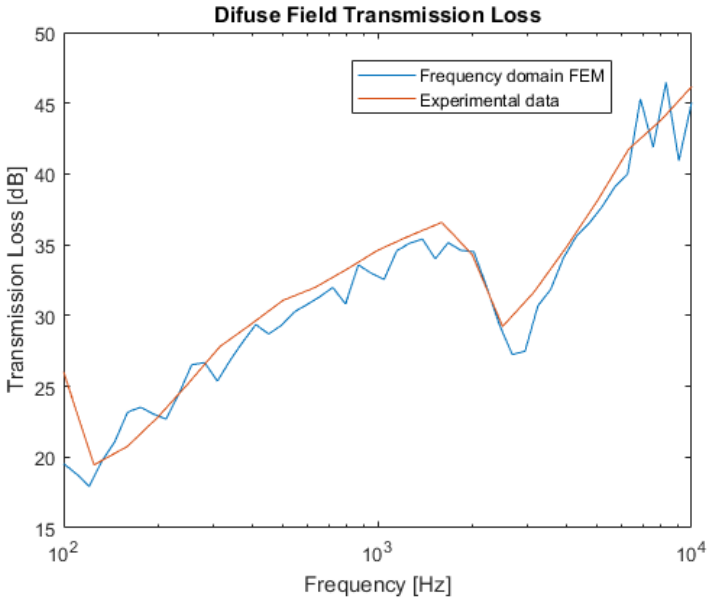

Figure 3 – Diffuse field Transmission Loss: numerical-experimental comparison.

A good match between the experimental and numerical TL over the whole frequency range (100-10000 Hz) is shown. In particular, the region around the critical frequency f_c=2.5 kHz is correctly caught as well as the low frequency range dependent on both the panel mass and the boundary conditions. A slight underestimation of damping can be observed at the critical frequency, this is mainly due to the absence of structural damping and the presence of ideal boundary conditions in the numerical model.

4. DESIGN AND APPLICATION OF AN ACTIVE CONTROL SYSTEM

In order to enhance the TL performance of the panel, Equation 7 is rewritten including an active control term

$$[M]\underline{\ddot{q}} + [C_F]\underline{\dot{q}} + [K]\underline{q} = 2\rho\underline{\dot{I}} + \varphi^T[B_c]\underline{F_c} \tag{12}$$

where the vector $\underline{F_c}$ contains the feedback forces. In Equation 10 $\varphi^T[B_c]$ is a matrix whose elements correspond to the modes evaluated at the forcing points. Equation 12 in state space form becomes

$$\underline{\dot{z}} = \begin{bmatrix} -[M]^{-1}[C_F] & -[M]^{-1}[K] \\ [I]_{NxN} & [0]_{NxN} \end{bmatrix}\underline{z} + \begin{bmatrix} 2\rho[M]^{-1} \\ [0]_{NxN} \end{bmatrix}\underline{\dot{I}} + \begin{bmatrix} [M]^{-1}\varphi^T[B_c] \\ [0]_{NxM} \end{bmatrix}\underline{F_c} \tag{13}$$

where $\underline{z} = \begin{bmatrix} \underline{\dot{q}} & \underline{q} \end{bmatrix}^T$ is the state vector, the first matrix is the state-space matrix, the second term is associated to the disturbance whereas the third term corresponds to the control contributions. Considering a feedback control law ($\underline{F_c} = [K_c]\underline{z}$), Equation 13 becomes

$$\underline{\dot{z}} = \left[\begin{bmatrix} -[M]^{-1}[C_F] & -[M]^{-1}[K] \\ [I]_{NxN} & [0]_{NxN} \end{bmatrix} + \begin{bmatrix} [M]^{-1}\varphi^T[B_c][K_c] \\ [0]_{Nx2N} \end{bmatrix}\right]\underline{z} + \begin{bmatrix} 2\rho[M]^{-1} \\ [0]_{NxN} \end{bmatrix}\underline{\dot{I}} \tag{14}$$

Different control algorithms can be adopted for computing the gain matrix $[K_c]$ depending on the objective to be reached. For instance, the IMSC control [17-18-19] is able to act directly on the damping and the stiffness of the plate keeping the mode shapes unaltered and the equations of motion decoupled. On the other side, the DMSC [15-16] modifies also the structure mode shapes, by exploiting a full gain matrix. This way it is possible to increase or reduce the energy introduced in the panel by the external disturbance.

Another well-known control algorithm is the LQR [20], where the gain matrix is derived by minimizing a cost function

$$J = \int_0^\infty \left(z^T Q z + {F_c}^T R F_c\right) dt \tag{15}$$

and considering the system dynamics (see Equation 13). The gain matrix is computed by solving the associated Riccati equation once defined the Q and R weighting matrices.

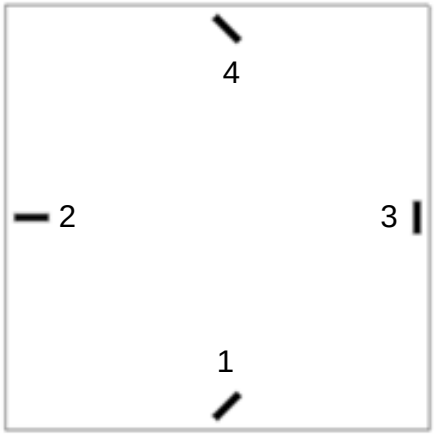

Figure 4 – Placement of the piezo-patch actuators for controlling the panel Transmission Loss.

In this work the LQR algorithm is applied with the aim of improving the Transmission Loss of the plate to an incoming perpendicular acoustic plane wave in the low frequency range (1-1000 Hz), where other passive solutions are less effective.

For the considered case, 4 piezo-patch actuators are placed on the panel as shown in Figure 4 and included in the model while, for the sake of simplicity, a direct feedback of the states is here considered. The design of the LQR control has been performed considering the first 72 modes covering the frequency range up to 1 kHz. The matrices Q and R are set to

$$Q = diag([1 \times 10^{12} \quad \cdots \quad 0 \quad 1 \times 10^{12} \quad \cdots \quad 0])$$
$$R = eye(4) \tag{16}$$

where R is the 4-by-4 identity matrix and Q has two equal sequences of 72 elements linearly decreasing from 1×10^{12} to 0. This way, the matrix Q aims at controlling mainly the lower frequency modes whereas in R all actuators are have the same weight. Once the gain matrix is computed, the full system is simulated accounting for the normal incident pressure wave disturbance. Figure 5 shows the comparison between the Transmission Loss for the passive and the controlled system.

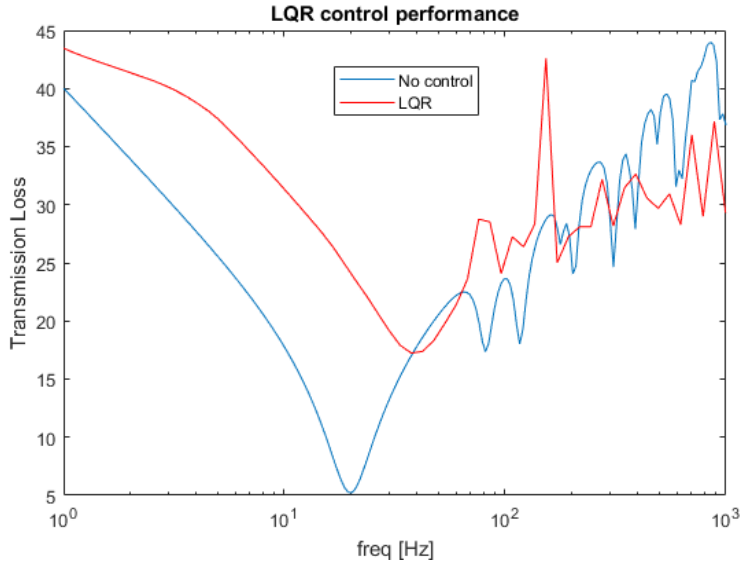

Figure 5 – Transmission Loss for the passive and controlled (LQR) panel in case of normal incident planar pressure waves.

It can be observed that a marked improvement is obtained for the controlled case at low frequency, especially around the first mode at 20Hz, where the TL is increased by 20 dB. An improvement of the performances is obtained up to approximately 200 Hz while the behaviour is similar to the passive case for higher frequencies, with a minimum effect of control spillover.

5. CONCLUSIONS

In this paper an active control solution, which aims at enhancing the sound Transmission Loss (TL) of lightweight panels, has been investigated. A numerical model of the panel, predicting the TL up to 10 kHz, has been implemented and validated against experimental data. The control law, based on the LQR algorithm, has been tuned in order to maximize its effects in the low frequency range, where passive solutions are generally less effective. A significative improvement in the panel performances has been observed up to 200Hz.

REFERENCES

1. N. Atalla, “Modeling the sound transmission through complex structures with attached noise control materials”, Wave Motion 51 (2014), 650-663
2. A. Mejdi, N. Atalla, S. Ghinet, “Wave spectral finite element model for the prediction of sound transmission loss and damping of sandwich panels”, Computers & Structures Volume 158 (2015), 251-258
3. Y. Yang, B. R. Mace, M. J. Kingan, “Wave and finite element method for predicting sound transmission through finite multi-layered structures with fluid layers”, Computers & Structures 204 (2018), 20-30
4. F. X. Xin and T. J. Lu, “Analytical and experimental investigation on transmission loss of clamped double panels: implication of boundary effects”, The Journal of the Acoustical Society of America 125 (2009), 1506-1517
5. S. Baro, R. Corradi, A. Parrinello and G. L. Ghiringhelli, “Numerical and Experimental Assessment of the Transmission Loss of Honeycomb Sandwich Panels”, Proceedings of INTER-NOISE 2018, Chicago, Illinois
6. T. Kaizuka N. Tanaka and K. Nakano, “Active control of sound transmission using structural modal filters”, Journal of Sound and Vibration 381 (2016), 14-29
7. Ripamonti, F., Baro, S., Molgora, M. Active vibration control for a smart panel with enhanced acoustic performances (2017) Proceedings of SPIE - The International Society for Optical Engineering, 10164, art. no. 101642W
8. A. Kundu A. Berry, “Active control of transmission loss with smart foams”, The Journal of the Acoustical Society of America 129 (2011)
9. R. L. Clark and C. R. Fuller, “Experiments on active control of structurally radiated sound using multiple piezoceramic actuators”, The Journal of the Acoustical Society of America 91 (1992), 3313–3320
10. X. Ma, K. Chen, S. Ding and B. Zhang, “Some physical insights for active control of sound radiated from a clamped ribbed plate”, Applied Acoustics 99 (2015), 1-7
11. V. Lhuillier, L. Gaudiller, C. Pezerat and S. Chesne, “Improvement of Transmission Loss Using Active Control with Virtual Modal Mass”, Advances in Acoustics and Vibration (2008)
12. U. Aridogan and I. Basdogan, “A review of active vibration and noise suppression of plate-like structures with piezoelectric transducers”. Journal of Intelligent Material Systems and Structures, 26 (2015), 1455-1476
13. V. Balamurugan, S. Narayanan, “Shell finite element for smart piezoelectric composite plate/shell structures and its application to the study of active vibration control”, Finite Elements in Analysis and Design, 37 (2001), 713-738
14. ISO 10140-1:2010 “Acoustics - Laboratory measurement of sound insulation of building elements - Part 1: Application rules for specific products”.
15. Serra, M., Resta, F., Ripamonti, F. Dependent modal space control: Experimental test rig (2017) JVC/Journal of Vibration and Control, 23 (15), pp. 2418-2429.
16. Serra, M., Resta, F., Ripamonti, F. Dependent modal space control (2013) Smart Materials and Structures, 22 (10), art. no. 105004, .
17. Meirovitch, L., Baruh, H. Robustness of the independent modal-space control method (1983) Journal of Guidance, Control, and Dynamics, 6 (1), pp. 20-25.
18. Bagordo, G., Cazzulani, G., Resta, F., Ripamonti, F. A modal disturbance estimator for vibration suppression in nonlinear flexible structures (2011) Journal of Sound and Vibration, 330 (25), pp. 6061-6069.

19. Resta, F., Ripamonti, F., Cazzulani, G., Ferrari, M. Independent modal control for nonlinear flexible structures: An experimental test rig (2010) Journal of Sound and Vibration, 329 (8), pp. 961-972.
20. Willems, J.C. Least Squares Stationary Optimal Control and the Algebraic Riccati Equation (1971) IEEE Transactions on Automatic Control, 16 (6), pp. 621-634.